technical memorandum Daresbury Laboratory

DL/SCI/TM49E

A MULTIANODE MULTICHANNEL DETECTOR FOR ANGLE RESOLVED PHOTOELECTRON SPECTROSCOPY

by

T.S. PADMORE, H.A. PADMORE and K.M. ROBERTS, SERC Daresbury Laboratory

JULY, 1986

Science & Engineering Research Council

Daresbury Laboratory

A MULTIANODE MULTICHANNEL DETECTOR FOR ANGLE RESOLVED PHOTOELECTRON SPECTROSCOPY

by

T.S. Padmore, H.A. Padmore and K.M. Roberts

SERC Daresbury Laboratory, Dareebury, Warrington WA4 4AD, England

Abstract

A multianode muitichannel detector for angle resolved photoelectron spectroscopy has been developed. A short review of existing eystems is included along with a description of the deeign and construction of the detector. Initial test spectra of Ag(111) using a rare gas discharge lamp are presented.

SCIENCE AND ENGINEERING RESEARCH COUNCIL

DARESBURY LABORATORY

1. Introduction

Photoemission experiments have the following independent parameters: the frequency, polarieation and angle of incidence of the photons, the crystal face, orientation and surface structure of the crystal under investigation, and the exit angle and spin polarisation of the photoelectrons. The energy distribution curves (EDC) in angle resolved photoelectron spectroscopy (ARPES) change, often drastically if one of these parameters especially the frequency and polarisation of the photons and the photoelectrons exit angle, is varied and examination of the electronic bands of the crystal throughout the Brillouin zone is possible.

ARPES experiments are carried out under ultra high vacuum conditions. In thie work the photoemitted electron kinetic energies are measured with an energy dispersive hemispherical analyser. The electrons are transported, and accelerated or retarded to the analyser transmission energy, from the sample to the entrance aperture of the hemispheres, by a three element electrostatic lens. The hemispheres disperse the electrons which travel between them about the line in the exit plane which lies on a radius (Purcell 1938). Fig.1 shows a echematic of this process for the VSW (Vacuum Science Workshop) HA50 analyser used in this work.

Conventionally a channeltron electron multiplier is used as the electron detector accepting a fraction of the electrons through an aperture placed at the centre of the exit plane. The entrance and exit apertures define the energy resolution (Imhof et al 1976). The electrons which arrive on either side of thie exit aperture carry information related to other kinetic energy valuee of electrons photoemitted from the sample. Multichannel techniques collect these electrons too, allowing simultaneous analysis of several kinetic energy values. Electrons which arrive at the mean radius position have energy E_0, the transmission energy of the analyser. Electrons with lower initial kinetic energies are not focussed exactly at the entrance aperture (see, e.g. Hoyland et al 1986), but they are transported around the hemispheres and pulled towards the inner hemisphere. Similarly, those of higher initial kinetic energy end up nearer the outer hemisphere at the exit plane. The energy window W over a distance L in the exit plane can be calculated in theory from the equation of Imhof et al (1976):

$$\frac{W}{E_0} = 0.43 \frac{L}{R_0} + \frac{\alpha^2}{4}$$

where E_0 is the transmission energy, R_0 is the mean radius and α the angular spread of the electrons. Terms in α can be ignored for the purpose of this calculation since W is calibrated by experimental methods. For L = 18 mm W is 0.155 E_0.

If a range of energies $E_0 \pm W/2$ can be measured while the analyser voltages are set up for one kinetic energy value then the increase in sensitivity is obvious. Such an increase is needed in photoemission experiments where spectra from surfaces, which are sensitive to contamination from the residual vacuum must be accumulated quickly. Apart from the ability to obtain spectra more quickly a multichannel system can be used to measure signals which are low relative to the background. Multiscanning of such a feature results in a high overall count rate with an increased signal-to-noise ratio over single channel counting. Bright photon sources are available, e.g. synchrotron or rare gas discharge lamp, so the development of a high count rate, e.g. 10^6 Hz capability, increased sensitivity detector for electrons is essential for the production of good statistical spectra from stable samples. Such a development opens up new avenues of research for photoemission experiments where the spectrum is superimposed on a large secondary background.

2. The Basic Multichannel Assembly

Electrons arriving in the exit plane need to be multiplied. The available gap between the inner and outer hemispheres is 28 mm for the HA50. One possible way of achieving parallel detection would be to instal several single channel detectors across the exit plane; however, several channeltrons would not fit into such a small gap and would not be able to cope with count rates in excess of 1 MHz. A schematic diagram of the basic multichannel assembly is shown in Fig.2. The multiplication is achieved via a chevron pair of microchannel plates (Wiza 1979). The pulses of electrons leaving the microchannel plates are accelerated on to the collector, which is able to transmit these pulses to the outside of the vacuum chamber. Several types of collector have been manufactured to perform this function; a review of such collectors is given in the following section. Note that the positional information of the pulse is required for energy analysis.

3. A Review of Multichannel Detecting Systems

With the advent of microchannel plates (Wiza 1979) position sensitive particle counters have been constructed for the detection of low energy particles. The electron pulses are either measured directly (see, e.g. Daviel et al 1982) or indirectly (see e.g. MacDowell et al 1983). There are a number of possible detection techniques which are discussed as follows:

3.1. Photographic Plate

The simplest method for capturing an extended image is to use a photographic plate but this suffers many disadvantages such as low quantum efficiency, poor dynamic range and non-linearity. Most importantly the quantitative analysis of such data is inconvenient.

3.2. Electronic Techniques

After amplification by the channel plates the charge cloud initiated by the impinging electron must be registered with its position. There are three main classes of detection technique (i) charge division techniques, (ii) image scanning techniques and (iii) multiple electrode arrays. These three techniques are discussed in the following subsections.

3.2.1. Charge Division Techniques

The charge cloud impinges on the resistive anode (collector) and divides. The arrival position is determined from the pulses detected at each end of the anode (Lampton and Paresce 1974). For one-dimensional readout the resistive strip forms an R-C line, which has the property that the decay time of the charge pulse depends on the position of excitation on the R-C line (Mathieson et al 1974). High spatial resolution of 50 μm has been obtained by Parkes et al (1974). This technique is fine for maximum count rates of 10 kHz per square centimetre but for many photoemission experiments this would be a severe limitation. The principal disadvantage of charge division systems is the large dead time, typically 0.5-5 μs which makes the system prone to pulse pile-up, especially for count rates greater than 2 kHz. This therefore limits the usefulness of this technique to instruments having low overall count rates where full advantage can be taken of its potentially high resolution with increased sensitivity (see, e.g. MacDowell et al 1983). Other charge division techniques have been developed by Wijnaendts van Resandt and Los (1979) and Gabriel et al (1978).

3.2.2. Image Scanning Techniques

An array of photo-sensing or charge-sensing detector elements is placed in the image field of the particles to be detected. Each element of the array consists of a small charge storage cell or capacitor. If a quantity of charge is deposited in one of these cells it remains stored in that location until it is neutralised or transferred elsewhere. After an interval of time, the stored charge pattern is read out in the form of an electricl signal presenting the positional information. Ideally the time taken to read out should be much less than the integration time to minimise the system dead time. Image scanning detectors can be divided into two groups: those employing television vidicon camera tubes and those using charge coupled devices. These image sensors are all photosensitive so a phospher screen is normally used to convert the charge pulses into photons. Vidicon tube type systems have been developed by Gelius et al (1973) and Caesar et al (1979). A problem with this type of detector is incomplete readout of the stored charge and further, the tube is physically bulky, making installation difficult. A charge coupled device system has been used successfully by Daviel et al (1982) for gas phase work. However for solid state photoemission the maximum count rate would be limited by the phosphor screen decay time which is of the order of milliseconds. This system would be fine for a fixed detector but for mounting on a three-axis goniometer fibre optic technology would have to be employed.

3.2.3. Multiple Electrode Arrays

Many independent anodes collect the charge pulses. Each anode is connected to a preamplifier and followed by a counter. A computer reads out the counters and constructs the positional and then energy distribution. This has the obvious advantage of a much higher maximum count rate capability. The main disadvantage from the point of view of some experimenters is the large quantity of electronic equipment required to process the signals from the detectors. This is a valid argument for those who expect low ($< 10^4$ Hz) overall count rates across the multidetector and hence use of one of the two methods previously described would be in order. Nilsson et al (1972) have described a discrete device consisting of parallel plate electron multipliers as the amplifying devices. The pulses are recorded after a capacitor placed at the exit of the multiplier. The noise level is low and the resolution good but the technique is laborious at both manufacture and readout stages.

The method chosen in this work was that of discrete anodes each with their own preamplifier and counting electronics preceded by a 25 mm pair of channel plates (Mullard G12-25 SE/A). It is in principle a simple arrangement and has the high count rate potential required with an increase in sensitivity over single channel counting.

4. The Design and Construction of the Multianode

The multianode was made by photoetching the design onto a copper-coated ceramic substrate. The existing exit assembly on the HA50 allowed for a substrate 60 mm in diameter, around which up to 40 connection holes could be drilled. The active area of the channel plates was 18 mm so this was chosen as the dispersion length. The films for photoetching were designed on a computer-aided design (CAD) system at Daresbury and can be seen in Fig.3. Each anode is 3 mm perpendicular to the plane of dispersion, being 225 μm wide with a 225 μm gap. There are 40 anodes in the 18 mm dispersion length. The reverse side of the substrate was also coated to enable biasing at the same potential as the anodes, the negative of which is shown in fig.3. For reduction of cross talk a ground plane (at H.T.) was constructed around the tracks leaving a small insulation gap. The lower limit for anode width is set by the maximum spread of electrons at the second microchannel plate. For the potentials applied (Fig.2), a maximum spread of eight channels, each 12.5 μm wide, can be expected. This sets ths lower limit at 100 μm.

A schematic layout of the electronics network is shown in fig.4. The multianode was connected in vacuum by some non-magnetic stainless steel barrel connectors and 75 Ω coaxial cable RG179 B/U, manufactured by Habia Ltd. Ceramaseal MHV feedthroughs were used on the flange. Outside vacuum RG 59 B/U, also 75 Ω, was used to connect up to the preamplifier.

5. Data Acquisition

The system requirements could be split into two sections; a 40-channel amplifier/discriminator processing the pulses from the multianode and a high epeed 40-channel scaler system to count the pulses from the discriminator. The 40 channels of scaler were very conveniently provided using the LeCroy "ECL line" 32-channel scalers (model 4434). These units required a differential ECL input and are sited in a standard CAMAC crate/LSI 11/23 system. The amplifier/discriminator system was designed and produced in-house by the

Instrumentation Lab. To allow for expansion it provided 48 channels of input and was a self-contained crate. The amplifier inputs contained the necessary bias and blocking components to operate the input at a d.c. potential of up to 3 kV (Fig.5). The channels were grouped in blocks of eight in double height euro-modules. Because of the problems of EHT distribution, the bias supply had to be provided separately for each block of eight amplifiers (Fig.6). A common discriminator threshold for all 48 channels was provided with a single multi-turn control. In addition, for test purposes a single common charge injection test input was provided. A commercial modular power supply was used to provide the low voltage amplifier/discriminator supplies and LED monitors were included for fault diagnosis. The amplifier was of a common base type in order to give low noise and the required matching impedance. The discriminator had a differential threshold level buffered from the front panel control. The useable threshold input was 1 million to 50 million electrons. The matching between channels was ±(500,000 + 20% of threshold). The input impedance was 75 Ω.

6. Calibration and Initial Results

The energy window, W, was experimentally measured by setting the analyser voltages, via CAMAC output driver (FISHER 2411) and a Cooknell's programmable power supply unit for single channel scanning using one of the central channels (No.20). A cleaned Ag(111) crystal was used as the sample and single channel spectra of the Fermi edge were accumulated from channel 20 and a given other channel simultaneously. This gives information about the energy separation between anodes and this leads to calibration of W. For this work only the even-numbered anodes were used (No.2 to No.40). This corresponds to 20 anodes in an 18 mm dispersion length. A spectrum for channel 20 and channel 10 at E_0 = 10 eV is shown in Fig.7. The step size was 25 meV. Spectra were taken for all the even anodes and the energy separations measured. These energy differences were plotted vs. channel number and W measured for a given E_0. The results for E_0 = 10 eV are shown in Fig.8 giving $W = 0.160\ E_0$. This value for the dispersion was checked for E_0 = 2 eV and 5 eV. However, it was only found to be the same if the front of the first channel plate was set to the transmission energy voltage (E_0/e). There was evidence for extensive field penetration into the hemispheres when a voltage of 200 V was applied. The values of W for this case were significantly different, namely ~ 0.40 E_0 for E_0 = 2 eV, 0.24 E_0 for E_0 = 5 eV and 0.17 E_0 for E_0 = 10 eV. Once a significant change was noticed for the E_0 = 2 eV case V_1 was altered to the field-free value and data runs restarted. The value of 0.160 E_0 for W is in good agreement with the theoretical value of 0.155 E_0.

Since the dispersion was measured to be reasonably linear, the method of scanning adopted was relatively simple and required no correction for the variation in intensity across the channel plates. An averaging process was employed. The analyser voltages were scanned so that a spectrum was stepped across the multianode in energy steps corresponding to the energy width of one anode W', where W' is given by

$$W' = 0.16\ E_0/20$$

Thus each point on the final output spectrum was accumulated from 20 data values added together each value having been recorded for subsequent analyser voltage settings during the scan. For a complete spectrum from a chosen START value and FINISH value, where FINISH is chosen to be an integer multiple of W from START, the analyser starting voltages must be set up for a mean kinetic energy value corrsponding to START-W/2 and must end at FINISH+W/2. This ensures that each point in the final spectrum is an accumulation of 20 data values. However, for a spectrum which is only W wide the scan will be relatively inefficient compared with a spectrum containing several windows (W). The expense of having to scan for an extra W in kinetic energy is more than compensated for by the increase in count rate achieved by the multidetector.

An example which shows the increase in sensitivity of the present multidetector is shown in Fig.9. The sample is Ag(111) and the spectra were taken at normal emission with an angular acceptance of ±1° FWHM at $\hbar\omega$ = 21.22 eV. The sample was cleaned by the usual method of argon ion bombardment at 2 keV followed by annealing to 700°C. Each spectrum took 16 mins to accumulate. The transmission energy was 2 eV. Note that the $\bar{\Gamma}$ surface state at the Fermi edge (E_F) is enhanced in the multichannel scan. The increase in sensitivity is 20.

As a check of the energy calibration a spectrum of the $\bar{\Gamma}$ surface state

using Ne I radiation (16.848 eV) was taken (Fig.10). The Ne I line has a spin orbit partner at 16.670 eV so spectral features should be separated by 0.178 eV. The surface state peaks from the two Ne lines are separated by 0.165 eV in good agreement with the expected value. The step size for the scan was 16 meV, corresponding to an anode-spacing width of 0.9 mm.

Acknowledgements

We would like to thank Dr. D. Norman and Dr. G. Thornton for their advice during this work and the following for their help on individual parts of the project: Mr. R. Lowery (mechanical engineering), Mr. M. Enderby and Dr. E.Pantos (computer software), and Mr. T. Weston (CAD).

References

Caesar G P, Weber J, Talmi Y, Surf. Interface Anal. 1, (1979) 45.

Daviel S, Hicks P J, Wallbank B, Comer J, Nucl. Instrum. Meth. 195, (1982) 323.

Gabriel A, Dauvergne F, Rosenbaum G, Nucl. Instrum. Meth. 152 (1978) 191.

Gelius U, Basilier E, Svensson S, Bergmark T, Siegbahn K, Uppsala Univ. Inst. Phys. Rep. No.817 (1973).

Hoyland M, Padmore H A, Jordan R, Padmore T S, Daresbury Lab. Tech. Memo. No.DL/SCI/TM44E (1986).

Imhof R E, Adams A, King G C, J. Phys. E: Sci. Instrum. 9, (1976) 138.

Lampton M, Paresce F, Rev. Sci. Instrum. 46, (1974) 1615.

MacDowell A A, Hillier I H, West J B, J. Phys. E: Sci. Instrum. 16, (1983) 487.

Mathieson E, Evans K D, Parkes W, Christie P F, Nucl. Instrum. Meth. 121, (1974) 139.

Nilsson P O, Jadrny R, Siegbahn K, Proc. Int. Conf. Spectrosc. Calif. USA ed. D.A. Shirley, (Amsterdam: North-Holland, 1972) p.141.

Parkes W, Evans K D, Mathieson E, Nucl. Instrum. Meth. 121, (1974) 151.

Purcell E M, Phys. Rev. 54, (1938) 818.

Wijnaendts van Resandt R W, Los J, Phys. Today, 163, (1979).

Wiza J L, Nucl. Instrum. Meth. 162, (1979) 587.

Figure Captions

Fig.1. Schematic diagram of the hemispherical analyser.

Fig.2. Basic multichannel assembly.

Fig.3. Front and back films for photoetching.

Fig.4. Schematic layout of the electronics.

Fig.5. EHT bias distribution.

Fig.6. EC705 crate system.

Fig.7. E_0 = 10 eV Ag(111) Fermi edge scan. (o) channel 10; ([]) channel 20.

Fig.8. E_0 = 10 eV calibration curve.

Fig.9. Multichannel and single channel spectra of Ag(111).

Fig.10. Ne I normal emission Ag(111) for E_0 = 2 eV.

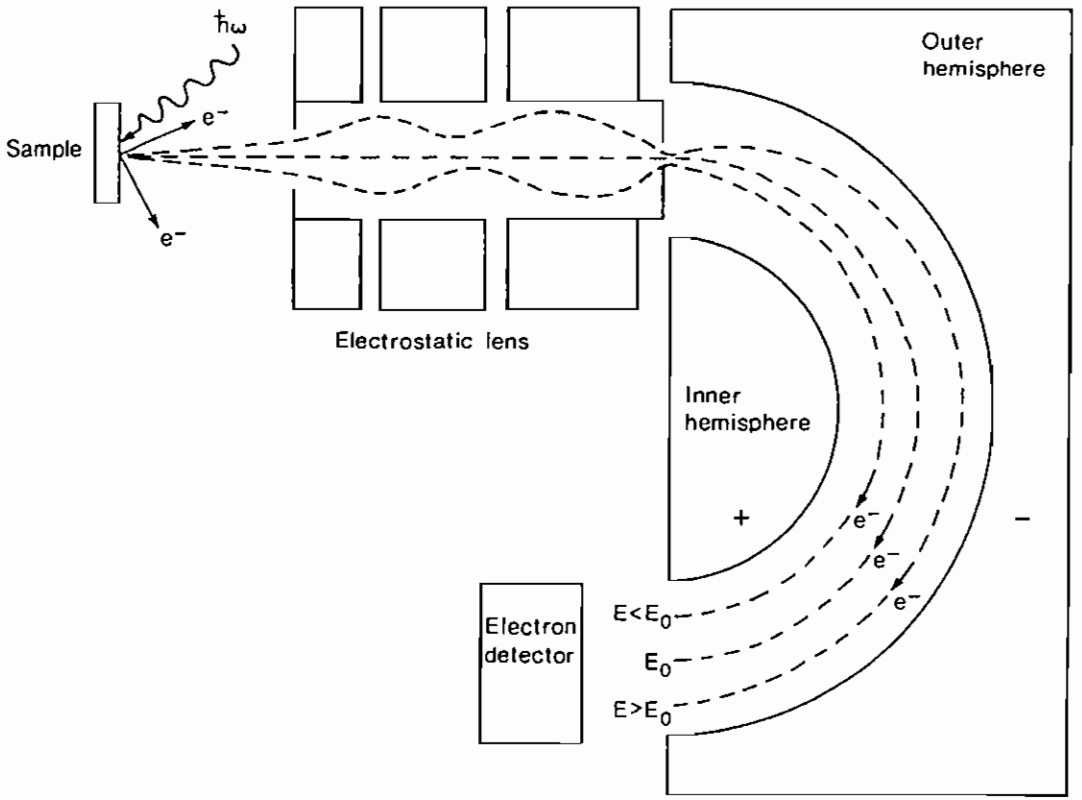

Fig. 1

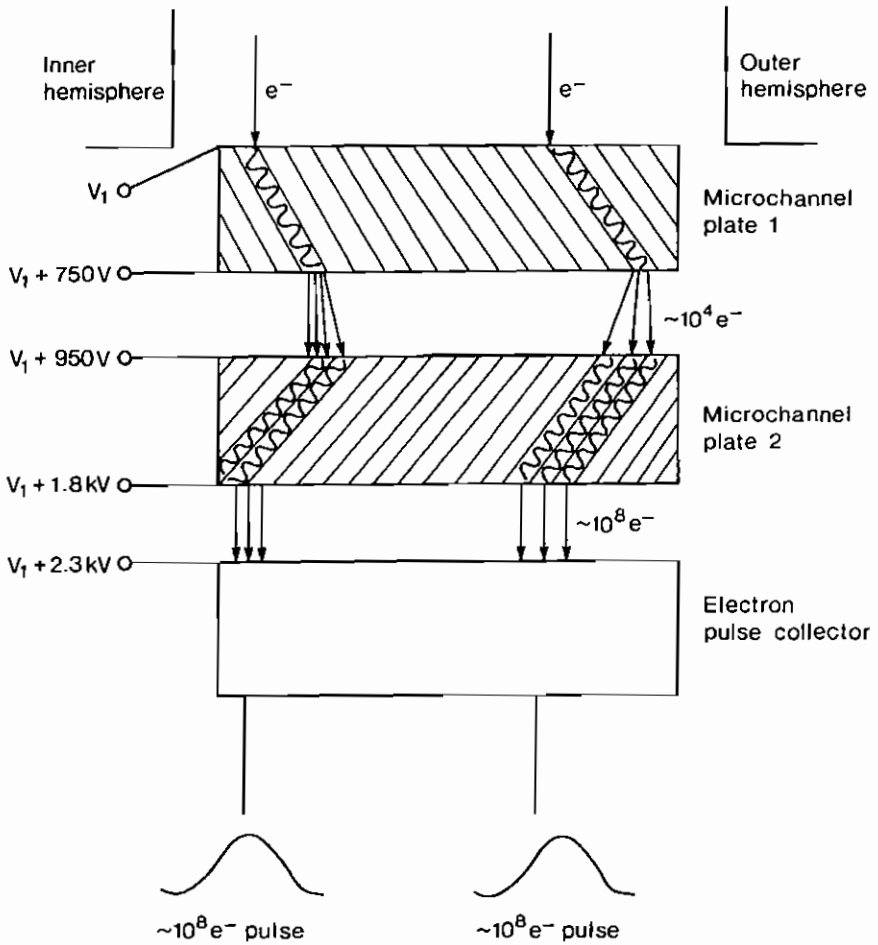
Inner hemisphere
e⁻
e⁻
Outer hemisphere
V1
Microchannel plate 1
V1 + 750V
~10⁴e⁻
V1 + 950V
Microchannel plate 2
V1 + 1.8kV
~10⁸e⁻
V1 + 2.3kV
Electron pulse collector
~10⁸e⁻ pulse
~10⁸e⁻ pulse

Fig. 2

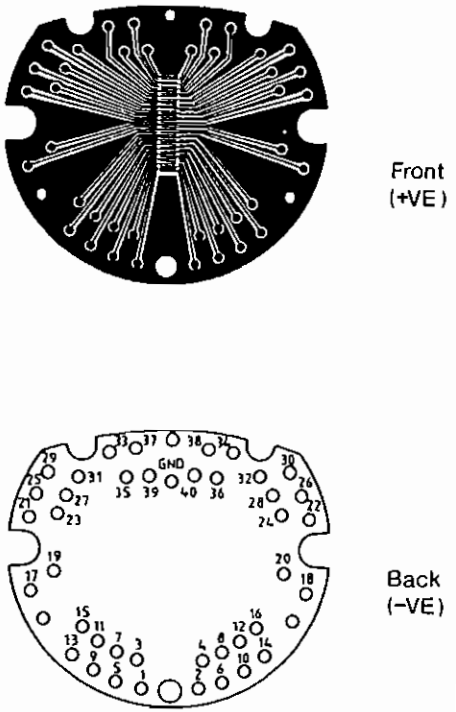
Front (+VE)
GND
Back (−VE)

Fig. 3

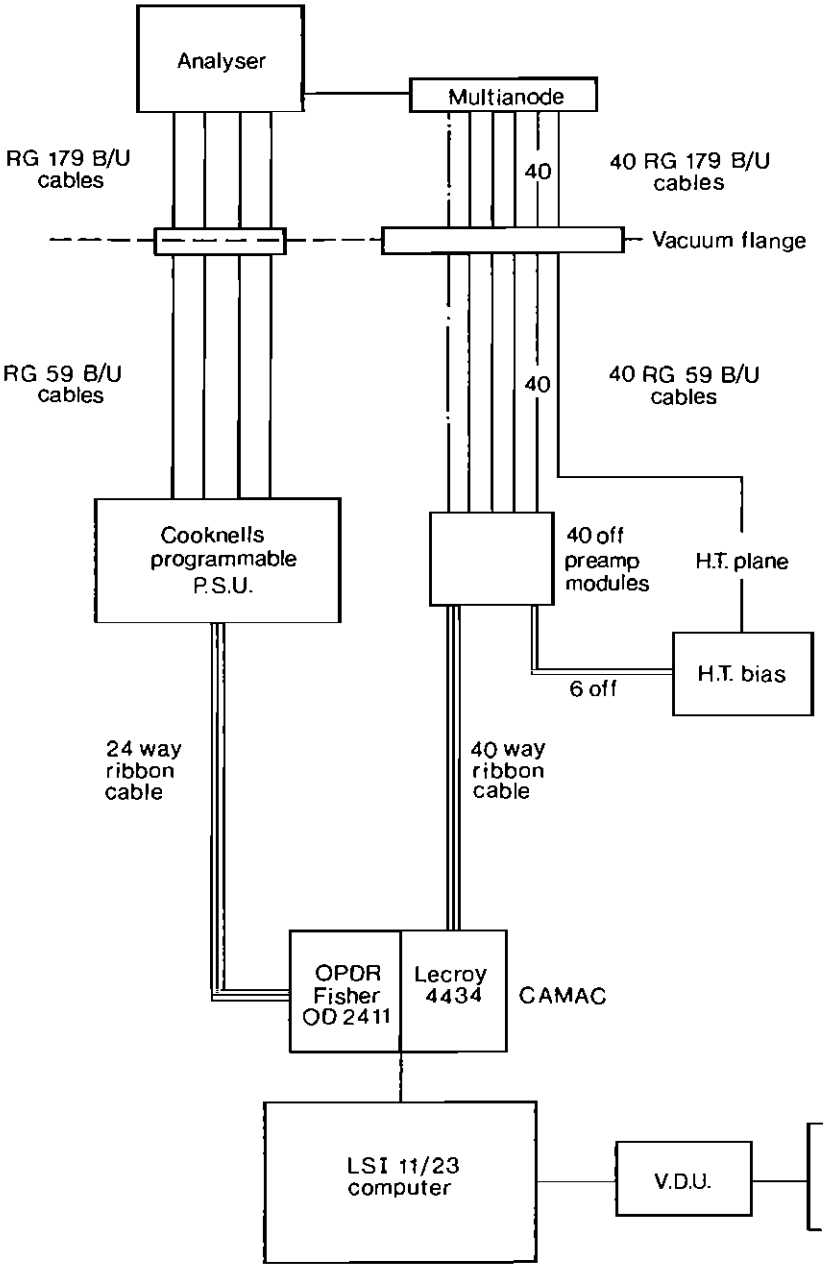

Fig. 4

The bias is commoned in blocks of eight channels

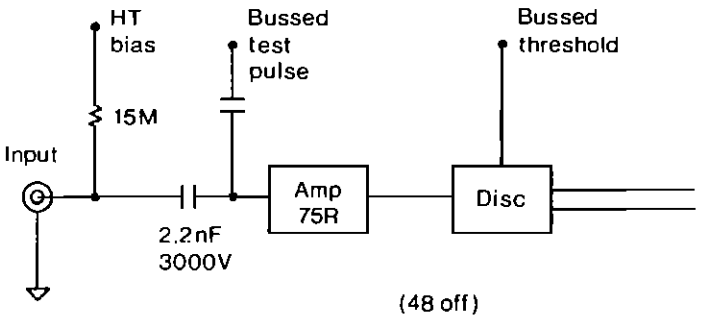

Fig. 5

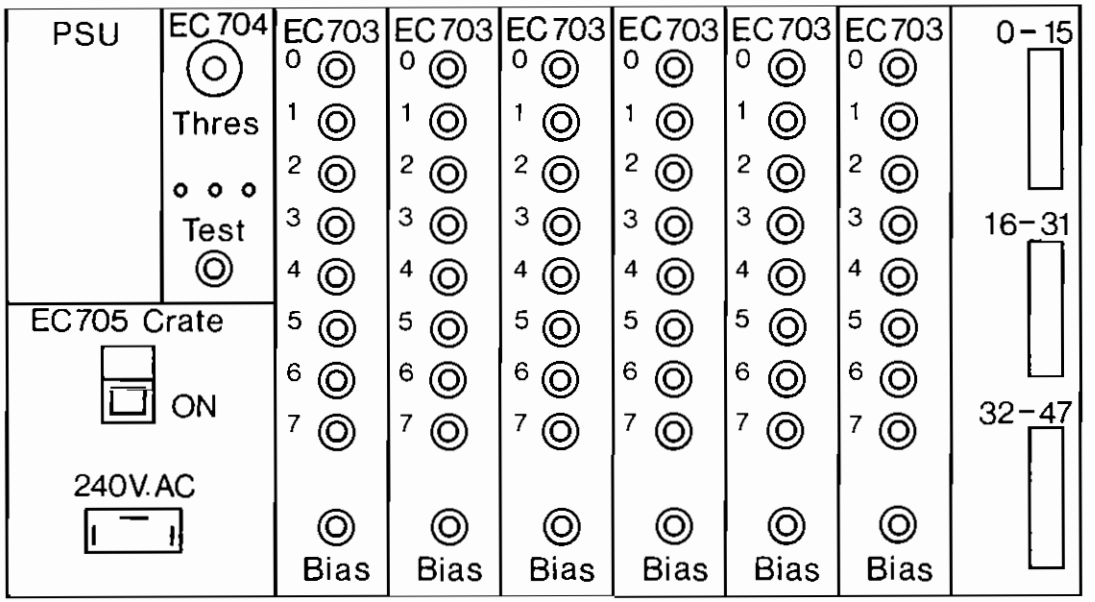
PSU
EC704
Thres
Test
EC705 Crate
ON
240V.AC
EC703
0
1
2
3
4
5
6
7
Bias
0-15
16-31
32-47

Fig. 6

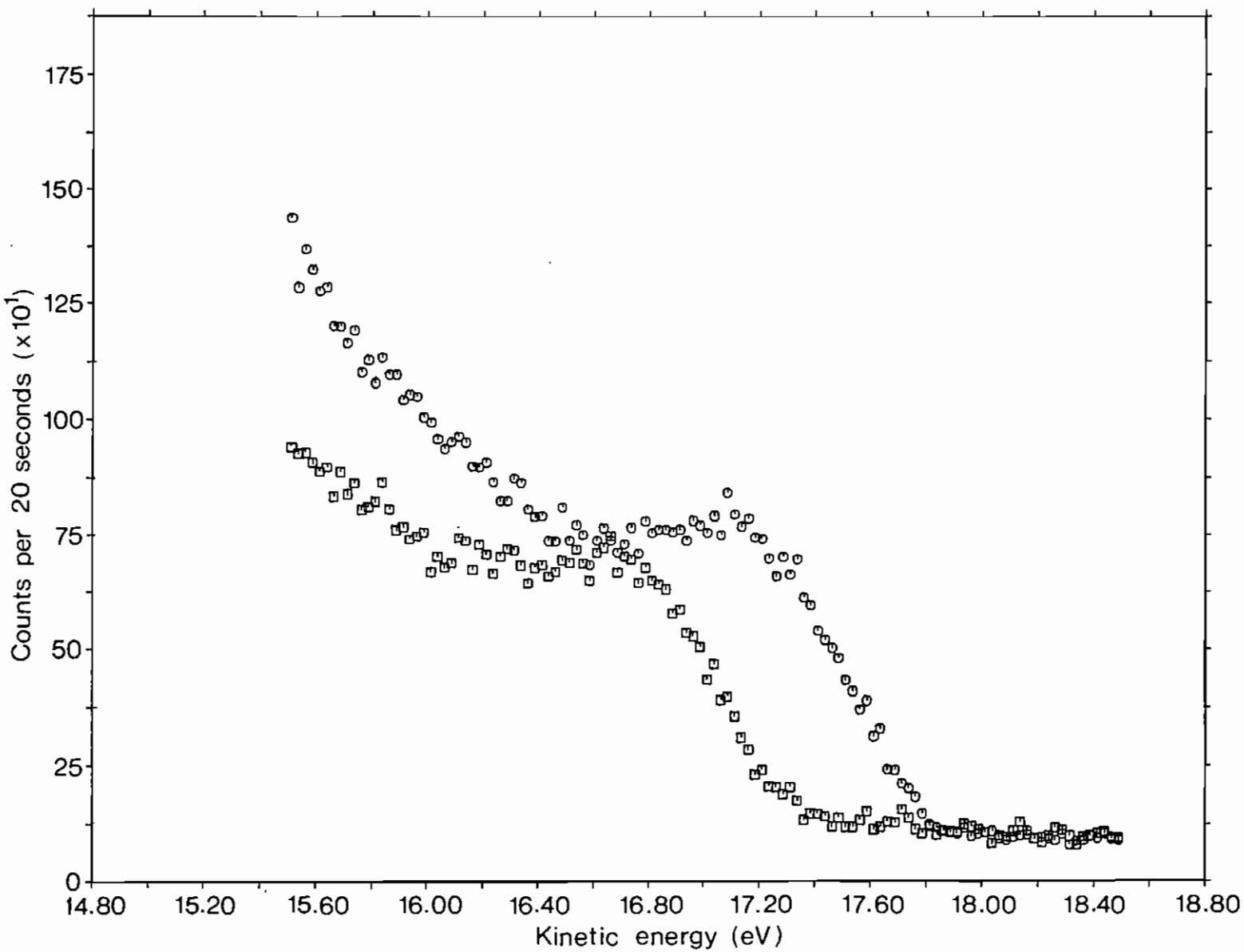
175
150
125
100
75
50
25
0
Counts per 20 seconds (x10¹)
14.80
15.20
15.60
16.00
16.40
16.80
17.20
17.60
18.00
18.40
18.80
Kinetic energy (eV)

Fig. 7

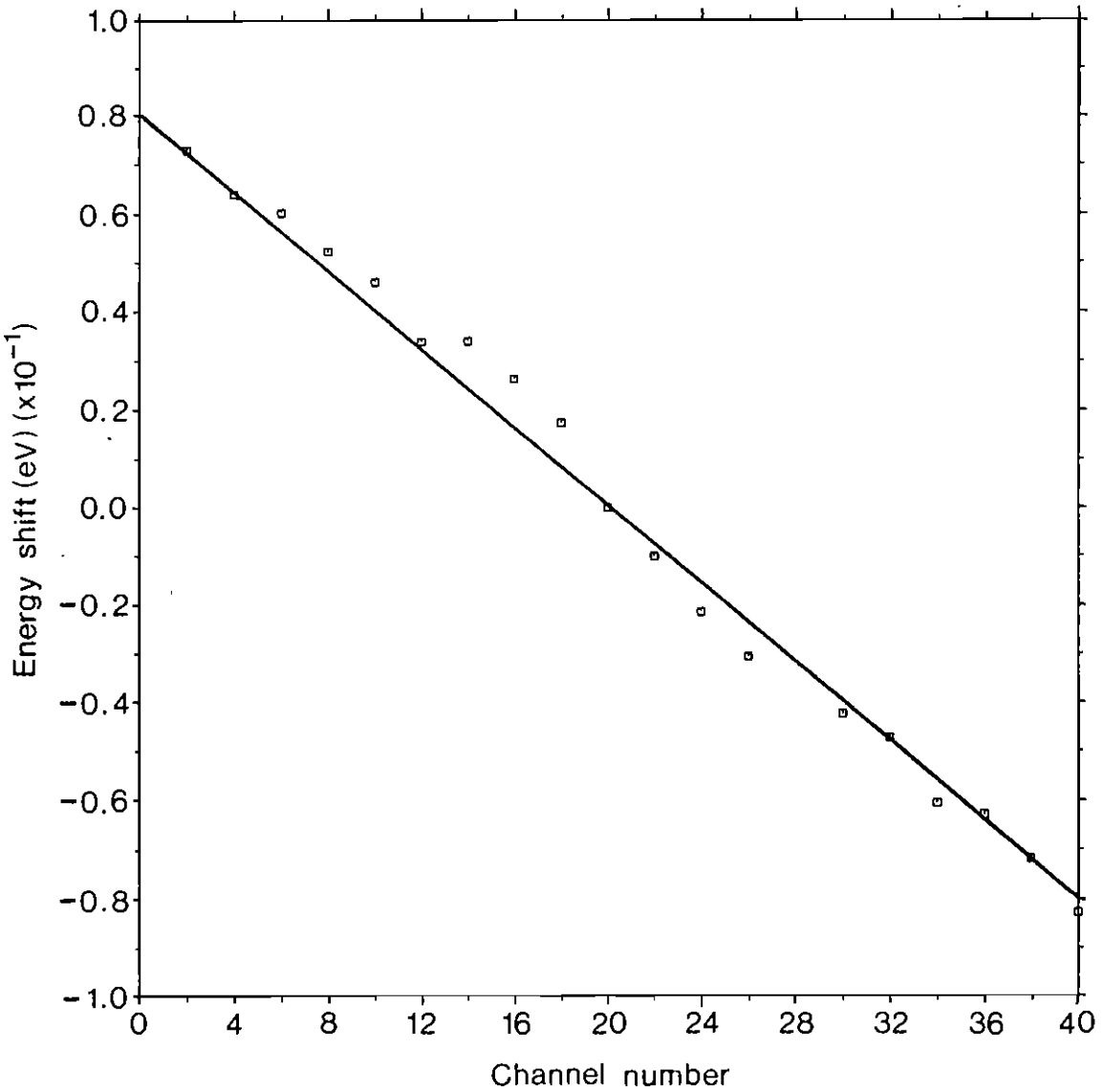
1.0
0.8
0.6
0.4
0.2
0.0
−0.2
−0.4
−0.6
−0.8
−1.0
Energy shift (eV) (x10^{-1})
0
4
8
12
16
20
24
28
32
36
40
Channel number

Fig. 8

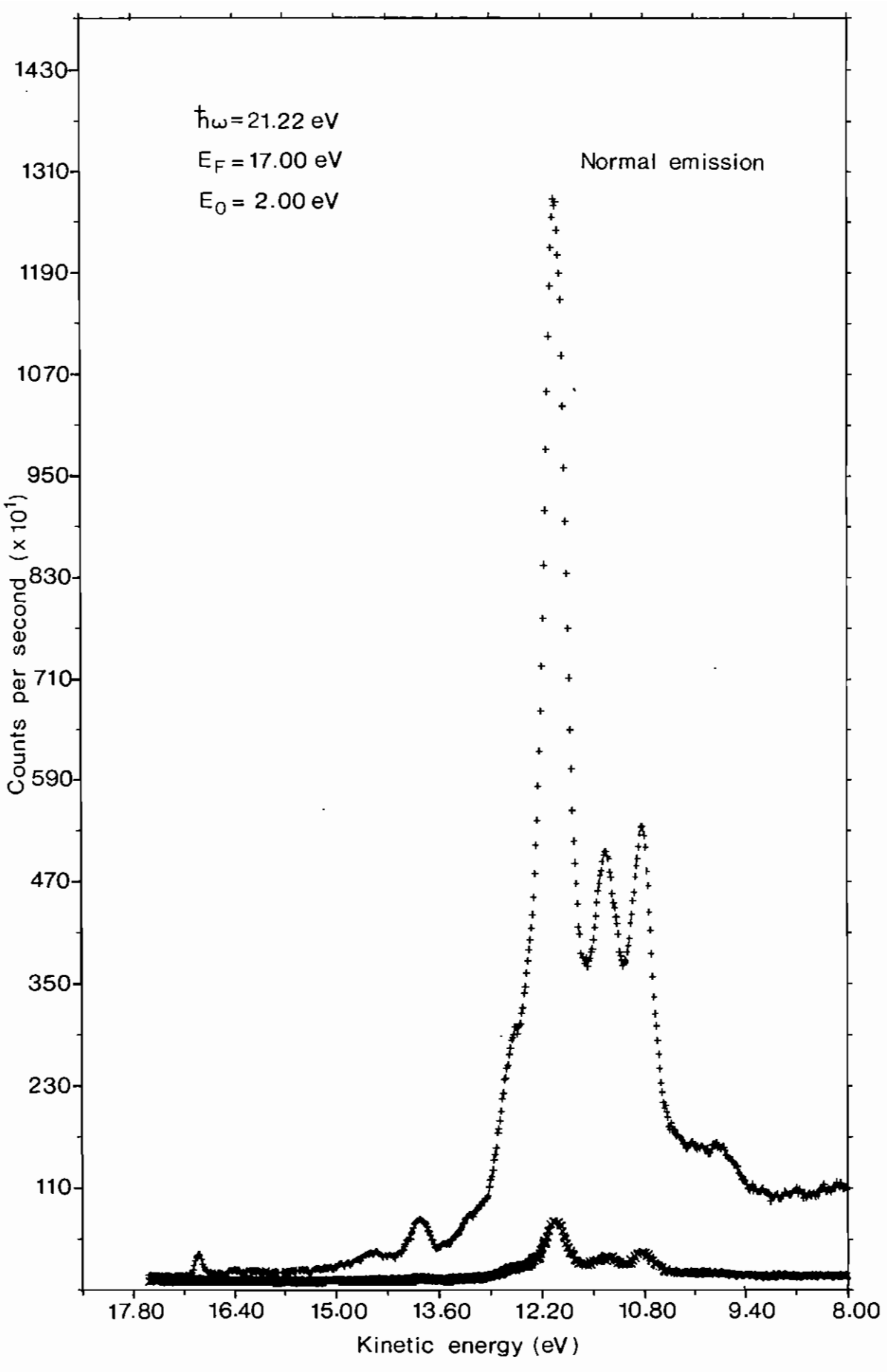
ħω = 21.22 eV
E_F = 17.00 eV
E_0 = 2.00 eV
Normal emission
1430
1310
1190
1070
950
830
710
590
470
350
230
110
Counts per second (x 10^1)
17.80
16.40
15.00
13.60
12.20
10.80
9.40
8.00
Kinetic energy (eV)

Fig. 9

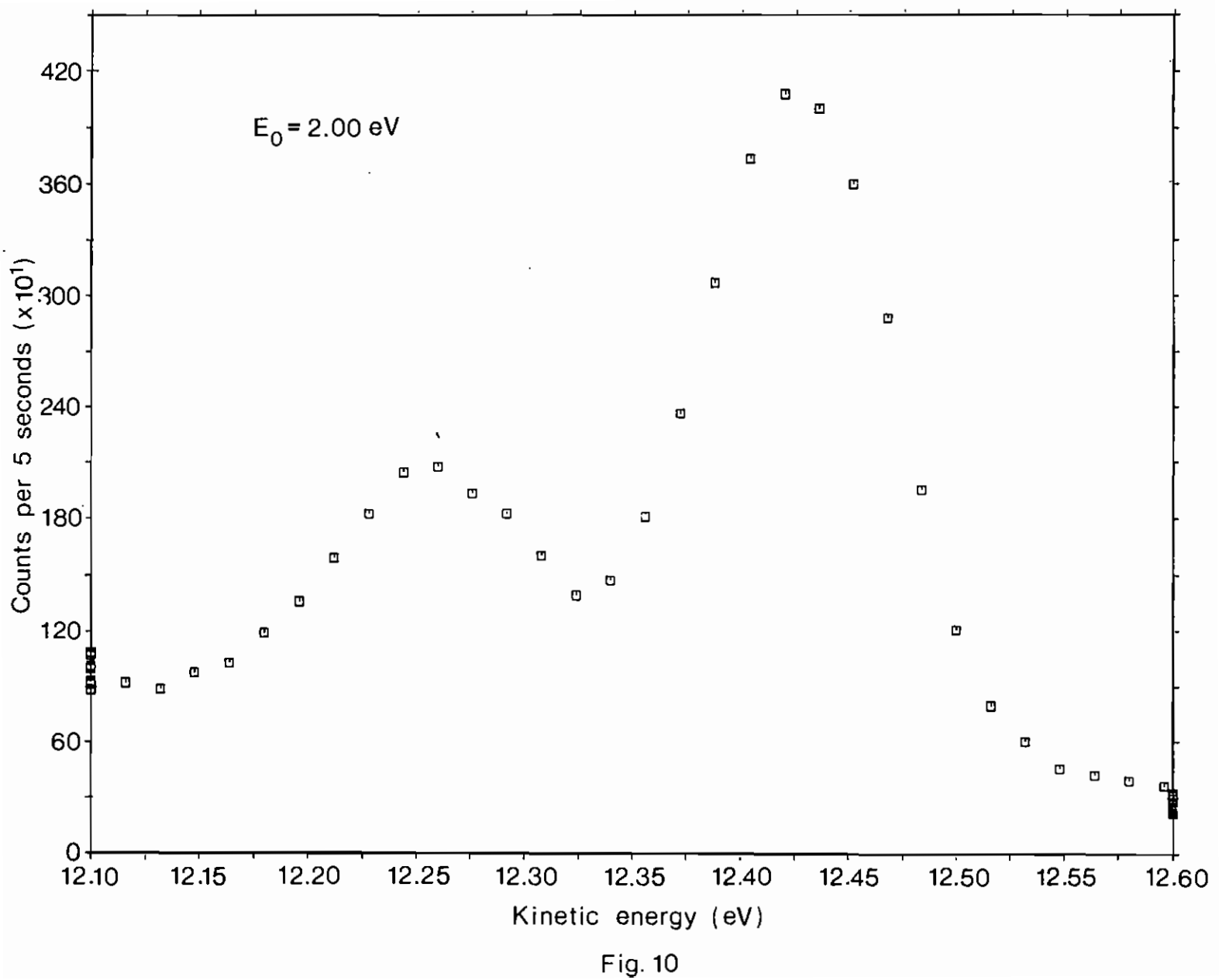
E_0 = 2.00 eV
Counts per 5 seconds (x10^1)
420
360
300
240
180
120
60
0
12.10
12.15
12.20
12.25
12.30
12.35
12.40
12.45
12.50
12.55
12.60
Kinetic energy (eV)

Fig. 10